Twenty-One New Theoretically Based Cubic Equations of State for Athermal Hard-Sphere Chain Pure Fluids and Mixtures

Arthur S. Gow and Robert B. Kelly*
Dept. of Chemistry and Chemical Engineering, University of New Haven, West Haven, CT 06516

DOI 10.1002/aic.14757
Published online March 11, 2015 in Wiley Online Library (wileyonlinelibrary.com)

Eight new hard-sphere equations of state (EOS's) were obtained from molecular simulation data for the pair correlation function $g_{HS}(\sigma)$ vs. packing fraction η and combined with three theoretical schemes to obtain 21 new cubic EOS's for athermal hard-sphere chains (AHSC's). The eight new hard-sphere EOS models successfully reproduced isotropic fluid compressibility factor Z_{HS} and $g_{HS}(\sigma)$ vs. η simulation data and predicted metastable liquid Z_{HS} vs. η and virial coefficients up through B_{10}. Moreover, calculated Z vs. η and reduced second-virial coefficient vs. chain length m were compared with molecular simulation data for chains up to $m = 201$ for a set of representative (eight of twenty-one) chain equations. Z vs. η for three AHSC binary mixtures was also successfully predicted. The results indicate that the new cubic EOS's give a satisfactory representation of simulation data for chain fluids and can be used to develop theoretically based cubic EOS's for "real" fluids including attractive effects. © 2015 American Institute of Chemical Engineers *AIChE J*, 61: 1677–1690, 2015

Keywords: thermodynamics/statistical, equation of state, molecular thermodynamics

Introduction

EOS's are essential tools for correlating, extrapolating, and predicting thermodynamic properties and phase behavior for pure fluids and mixtures. Considerable progress has been made in over a century in developing accurate theories[1–6] and EOS's [7–13] for small atomic or molecular fluids. The hard-sphere reference system is a good choice in perturbation theories for small molecules ranging from noble gases to hydrogen bonding fluids such as water. However, several classes of substances such as high molecular weight alkanes, polymers, proteins, surfactants, and ionic liquids are structurally complex molecules for which the hard-sphere reference model gives generally poor results when used in perturbation theories for thermodynamic property and phase equilibria calculations. A more accurate reference system for such fluids is the homonuclear athermal hard-sphere chain (AHSC) model, which accounts for intermolecular repulsion between spherical segments and intramolecular covalent bonding between adjacent rigid segments. Moreover, several workers[14–18] have given convincing arguments that fluid structure, especially at moderate-to-high densities, is predominantly determined by repulsive forces, and that attractive forces can be accurately represented by a weaker temperature- and density-dependent perturbation term. Thus, it is advantageous to develop models for chain fluids for which repulsive and covalent bonding (attractive) effects dominate. Finally, from a computational standpoint, it is beneficial to derive equation of state (EOS) models that are overall cubic in molar volume (i.e., have three real roots or one real root and two complex conjugate roots).

Several elements go into developing accurate theoretically based cubic chain fluid EOS models. First, a theoretical framework that expresses the fluid total Helmholtz free energy or compressibility factor as a combination of repulsion and bonding effects is required. Much work has been done in recent decades to advance the thermodynamic theory and development of EOS's for chain fluids and is excellently reviewed.[13,19] Three main theoretical platforms have been advanced for athermal chains: (1) thermodynamic perturbation dimer theory (TPT-D),[20,21] (2) hard-sphere-chain (HSC) theory,[18,22,23] and (3) generalized Flory dimer (GFD) theory.[24,25] Computational details for these platforms are presented in the next section of this article.

Furthermore, a suitable hard-sphere EOS is required to model repulsions between spherical segments. Some common functional forms are identified by reviewing the EOS literature. These forms, the van der Waals/Scott (vdWS), Percus–Yevick/Deiters (PYD), and nonfactorable quadratic (NFQ) forms, are shown to be reducible to a single simple functional form, which is cubic in molar volume. Below, we present general criteria (including the concept of thermodynamic correctness) for hard-sphere cubic EOS development and propose eight new thermodynamically correct cubic HS EOS's. These models can be used as templates for the development of EOS's which incorporate other effects including chain formation.

Finally, each of the TPT-D, HSC, and GFD theoretical platforms requires a bonding compressibility factor contribution. The TPT-D bonding term is directly obtained from Z_{HS}.

**Present address:* Dept. of Chemical Engineering, University of Rhode Island, Kingston, RI 02881

Additional Supporting Information may be found in the online version of this article.

Correspondence concerning this article should be addressed to A. S. Gow at agow@newhaven.edu.

The bonding contributions for HSC and GFD are refit forms of the Percus–Yevick hard-sphere pair correlation function at contact $g_{HS}^{PY}(\sigma)$ and Z_{DB} from the hard-dumbbell fluid EOS, respectively. Moreover, TPT-D also requires the fluid hard-dimer site-site correlation function at contact $g_{HD}(\sigma)$. It is significant that in each case developed in this article, the same polynomials used in the Z_{HS} expression are maintained in all auxiliary functions, resulting in cubic EOS's. The details of how these terms are obtained are given later in this article.

We apply this comprehensive approach to derive 21 new molecular-based cubic EOS's for AHSC fluids. Our approach is the first to our knowledge that combines the aspect of a general theoretical framework for chain fluids (e.g., TPT-D, HSC, or GFD) with a generalized form of the hard-sphere fluid EOS. The combination of these aspects permits the derivation of several theoretically based cubic EOS's for athermal chain fluids that can serve as backbones for real fluid EOS's including attractive effects.

Theoretical Platforms for AHSC EOS Development

Wertheim[26,27] proposed a comprehensive theory for intermolecular association and covalent bonding between spherical segments within molecules. Chapman et al.[28] obtained a general expression for the compressibility factor Z^m of a chain molecule in terms of the packing fraction η

$$Z^m = mZ_{HS} - (m-1)\left[1+\eta\frac{\partial \ln g_{HS}(\sigma)}{\partial \eta}\right] \quad (1)$$

where m is the number of spherical segments in the chain, Z_{HS} is the compressibility factor of monomer segments, and $g_{HS}(\sigma)$ is the pair correlation function of monomers at contact value. The first term on the right-hand side of Eq. 1 is the hard-sphere repulsion contribution, whereas the second term is the bonding contribution. Implementation of Eq. 1 requires an expression for $Z_{HS} = Z_{HS}(\eta)$ for which $Z_{HS} = 1$ as $\eta \rightarrow 0$ (ideal gas limit). Once Z_{HS} vs. η is established, the required relationship for the pair correlation function $g_{HS}(\sigma)$ can be obtained by application of the pressure equation of statistical mechanics

$$g_{HS}(\sigma) = \frac{Z_{HS}-1}{4\eta} \quad (2)$$

Moreover, expressions for $g_{HS}(\sigma)$ should also meet the ideal gas requirement that $g_{HS}(\sigma) = 1$ as $\eta \rightarrow 0$. Equation 1 with the noncubic hard-sphere EOS of Carnahan and Starling[10] gives the repulsive and chain compressibility factor contributions in many variants of the popular statistical associating fluid theory EOS's.[19,29] While Eq. 1, which is known as first-order thermodynamic perturbation theory (TPT1), gives adequate results when compared with molecular simulation data for short-chain fluids, results deteriorate as chain length increases, which presents problems for longer chain molecules and polymers. Ghonasgi and Chapman[20] recognized that Eq. 1 could be formally generalized to apply to the case in which an r-mer is dimerized to form a 2r-mer. The main assumption in their theory is that the derivatives $\partial \ln g_{\alpha\gamma}^{r}(\sigma)/\partial\eta$ and $\partial \ln g_{\alpha\gamma}^{2r}(\sigma)/\partial\eta$ are equal where $g_{\alpha\gamma}^{r}(\sigma)$ is the r-mer end segment site-site correlation function. This leads to the general expression for the dimer perturbation theory (TPT-D)

$$Z^m = mZ_{HS} - \frac{m}{2}\left[1+\eta\frac{\partial \ln g_{HS}(\sigma)}{\partial \eta}\right] - \left(\frac{m}{2}-1\right)\left[1+\eta\frac{\partial \ln g_{HD}(\sigma)}{\partial \eta}\right] \quad (3)$$

The additional requirement for TPT-D is the intermolecular site-site hard-dimer pair correlation function at contact value $g_{HD}(\sigma)$. Theoretical and empirical relations[20,30,31] are commonly used, however, we show later that simple new forms are obtained from simulation data for both $g_{HS}(\sigma)$ and $g_{HD}(\sigma)$. Equation 3 (based on the dimer reference) has been shown to give better results than Eq. 1 for hard-sphere chain fluids.[20,21,32] Thus, TPT-D will be adopted here as one theoretical route to new cubic EOS development.

Another successful approach to develop hard-sphere chain EOS's is the hard-sphere chain (HSC) theory of Chiew and Prausnitz and coworkers.[18,22,23] The approach is usually referred to as perturbed hard-sphere chain theory because it typically considers the complete EOS applicable to real fluids including attractive interactions. We will use only the athermal part of this EOS framework and call it HSC theory. The general expression for the compressibility factor of a chain of length m, which is based on Chiew's[30] solution to the Percus–Yevick integral equation for pure chain fluids and mixtures, is

$$Z^m = 1 + m^2 b\rho g_{HS}(\sigma) - (m-1)\left[g_{HS}^{PY}(\sigma)-1\right] \quad (4)$$

where b is the van der Waals covolume, the packing fraction is expressed as

$$\eta = \frac{mb\rho}{4} \quad (5)$$

and the fluid density is given by ρ. There are two pair correlation functions in Eq. 4: the unrestricted hard-sphere pair correlation function $g_{HS}(\sigma)$, obtained from Eq. 2 and a suitable expression for Z_{HS} (e.g., the Carnahan–Starling (CS) EOS) and the Percus–Yevick hard-sphere pair correlation function $g_{HS}^{PY}(\sigma)$, which is obtained by considering connectivity constraints between segments in chains. Combination of Eqs. 2, 4, and 5 and subsequent rearrangement yields an equivalent form of the HSC theory

$$Z^m = mZ_{HS} - (m-1)g_{HS}^{PY}(\sigma) \quad (6)$$

It can be seen by comparing Eq. 1 for TPT1 and Eq. 6 for HSC theory that the terms for intermolecular segment repulsion are the same while the difference between the two theories is in the bonding term (however, TPT-D is an improved version of TPT1 that will be used in this article).

The third theoretical platform for hard-sphere chain cubic EOS development is the GFD theory, which was advanced by Hall and coworkers[24,25] during the 1980s. This framework is based on the osmotic EOS, which expresses the compressibility factor Z^m in terms of the probability of inserting a single chain of length m into a bulk fluid of chains of length m. The key issue in GFD is the choice of expression for the insertion probability, which depends on molecular structure. A suitable expression for insertion of a homonuclear straight chain has been determined by Hall and coworkers,[25,33] and when combined with the osmotic equation yields an analytical expression for Z^m

$$Z^m = (Y^m+1)Z_{DB} - Y^m Z_{HS} \quad (7)$$

where Z_{DB} is hard-dumbbell fluid compressibility factor and Y^m is given by

$$Y^m = 0.95926 + 0.95926(m-3) \qquad 2 \le m \le 8 \qquad (8)$$

or

$$Y^m = 12.22789 + 0.92715(m-15) \quad m > 8 \qquad (9)$$

Equations 7–9 can be used in the GFD approach with suitable expressions for Z_{HS} and Z_{DB}. Figure 1 outlines the computational scheme that is used to obtain chain fluid EOS's, the details of which are described in the following sections of this paper. We now define what constitutes an acceptable hard-sphere EOS that can be used with the above three theories (TPT-D, HSC, and GFD) to develop cubic EOS's for chain fluids.

Hard-Sphere EOS's: Design Criteria, Existing Forms, and New Proposals

As we have pointed out, knowledge of repulsive forces is paramount to understanding fluid structure, especially at high density. Moreover, an accurate and mathematically simple expression for hard-sphere compressibility factor vs. packing fraction (HS EOS) is required for the TPT-D, HSC, and GFD theories to yield a chain compressibility factor Z^m expression that is cubic in molar volume. Here, we outline a few general guidelines that aid in the design of a thermodynamically correct, accurate, and mathematically sufficient expression for Z_{HS}. We propose that an acceptable HS EOS has the following attributes:

1. The compressibility factor has the correct ideal gas limit ($Z_{HS} = 1$ as $\eta \to 0$).

2. The pair correlation function at contact value has the correct ideal gas limit [$g_{HS}(\sigma) = 1$ as $\eta \to 0$].

3. The EOS should have the correct high density packing fraction limit ($\eta_{max} = 0.74$, consistent with a face-centered-cubic lattice structure), yielding a more accurate representation of Z_{HS} vs. η in the metastable fluid region.

4. The second-virial coefficient has the theoretically correct value ($B_2 = 4$ from molecular simulation data). Higher virial coefficients should be as close as possible to those obtained from simulation.

5. A HS EOS (Z_{HS} vs. η) obtained from applying criteria (1) to (4) is mathematically constructed such that an overall cubic athermal chain EOS (Z^m vs. η) is obtained when one of the theoretical platforms (TPT-D, HSC, or GFD theory) is applied to the HS EOS.

6. A HS EOS, which is obtained from applying criteria (1) to (4) above should be (if possible) quadratic overall in molar volume, allowing mathematical degrees of freedom in obtaining an overall cubic EOS for a real fluid including attractive effects (more choices of bonding and attractive terms).

First, note that the above criteria are mainly divisible into thermodynamic constraints [(1)–(4)] and mathematical (practical) constraints [(5) and (6)]. We use the term thermodynamically correct (avoids confusion with thermodynamically consistent) to describe an equation which meets the first two requirements. Furthermore, note that this list of criteria has

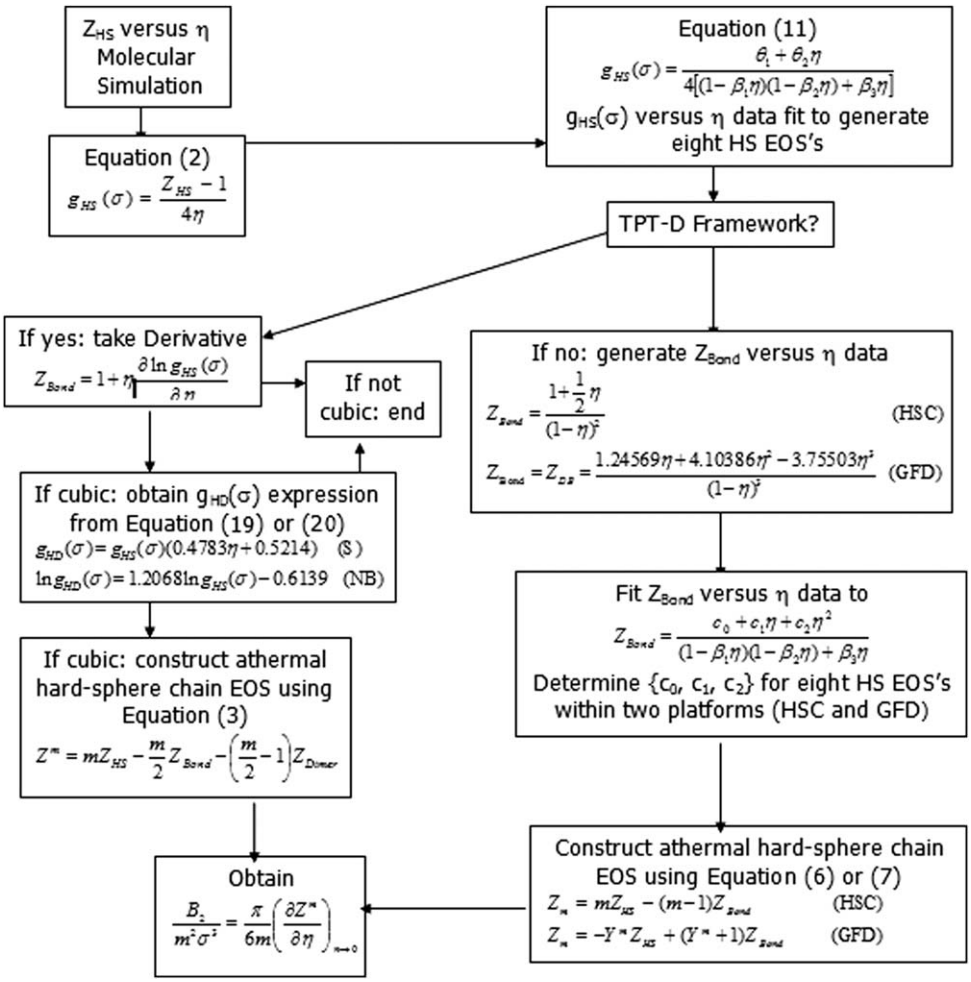

Figure 1. Computational steps for hard-sphere chain cubic EOS development.

been prioritized into items which are required (is) and items which are desirable (should be), reflecting that a simple cubic EOS will have some limitations and that "trade-offs" will exist. We will use the above list as a guide to assess published forms of HS EOS's and to propose new forms in this article.

Next, we present a universal HS EOS expression into which both published models of interest and new forms developed in this article can be cast. We have found that models from the literature, which are in fact cubic or are candidates for developing cubic EOS's, are special cases of a general hard-sphere EOS

$$Z_{HS}=1+\frac{\theta_1\eta+\theta_2\eta^2}{(1-\beta_1\eta)(1-\beta_2\eta)+\beta_3\eta} \tag{10}$$

where the β_i's and θ_i's are characteristic constants for a particular HS EOS.

Application of Eq. 2 to Eq. 10 yields the general expression for the hard-sphere pair correlation function at contact value

$$g_{HS}(\sigma)=\frac{\theta_1+\theta_2\eta}{4[(1-\beta_1\eta)(1-\beta_2\eta)+\beta_3\eta]} \tag{11}$$

First, note that "thermodynamic correctness" as we have defined it by criteria (1) and (2) in the list above only requires that $\theta_1=4$. Next, we have observed that published EOS's, which are described by Eq. 10, are divisible into four simpler subtypes of equations. We will refer to the first (simplest) class of equations as van der Waals/Scott1-type (vdWS1) EOS's which are of the form

$$Z_{HS}=\frac{1+k_1\eta}{1-k_2\eta} \tag{12}$$

with the corresponding contact value of the hard-sphere radial distribution function given by

$$g_{HS}(\sigma)=\frac{k_1+k_2}{4(1-k_2\eta)} \tag{13}$$

and with $\beta_1=k_2$, $\beta_2=\beta_3=0$, $\theta_1=k_1+k_2$ and $\theta_2=0$. One new thermodynamically correct vdWS1-type HS EOS is proposed in this work.

Furthermore, we classify mathematically slightly more complex models with the same denominator as in Eq. 12 and a quadratic dependence on packing fraction in the numerator as van der Waals/Scott2-type (vdWS2-type) hard-sphere EOS's. These EOS's are of the form

$$Z_{HS}=1+\frac{k_1\eta+k_3\eta^2}{1-k_2\eta} \tag{14}$$

and the pair correlation function at contact is thus

$$g_{HS}(\sigma)=\frac{k_1+k_3\eta}{4(1-k_2\eta)} \tag{15}$$

Note that Eq. 14 is a restricted case of Eq. 10 with $\beta_1=k_2$, $\beta_2=0$, $\beta_3=0$, $\theta_1=k_1$, and $\theta_2=k_3$. We later present one new thermodynamically correct version of this model.

All vdWS1- and vdWS2-type HS EOS's have a first-order packing fraction dependence in the denominator of Eq. 10. Another class of models that may be used to construct cubic EOS's has a quadratic dependence of packing fraction in the denominator of Eq. 10 ($\beta_1\neq 0$, $\beta_2\neq 0$, and $\beta_3=0$). These models are what we will call PYD type HS EOS's. Finally, we classify cases of Eq. 10 in which $\beta_3\neq 0$ as "NonFactorable Quadratic" (NFQ) EOS's because the denominator of polynomial degree two is only factorable by completing the square (i.e., $\beta_3>0$). The interesting possibility for this class of EOS's is that roots for η in the denominator may be complex resulting in no existing packing fraction pole. One new NFQ-type HS EOS is presented later.

The overall goal of this work is to develop models that approximate the noncubic CS EOS

$$Z_{HS}=\frac{1+\eta+\eta^2-\eta^3}{(1-\eta)^3} \tag{16}$$

and its corresponding pair correlation function

$$g_{HS}(\sigma)=\frac{1-\frac{1}{2}\eta}{(1-\eta)^3} \tag{17}$$

A brief historical perspective on the van der Waals and CS HS EOS's is given in Supporting Information Appendix A1.

The above classification of hard-sphere EOS's (according to different forms of Eq. 10) is based on a thorough examination of the HS EOS literature, the results of which are summarized in Tables 1 and 2. First, we note that several different approaches, including but not limited to, statistical mechanical theories, Padé approximants, and other closures to virial expansions, and fits of molecular simulation data for virial coefficients or compressibility factor were used to derive, design or construct all of the HS EOS's shown in Tables 1 and 2. Second, we observe that there are two basic forms of vdWS-type HS EOS's (vdWS1- and vdWS2-type models), which often have degrees of freedom in obtaining overall cubic EOS's when the bonding and attractive terms are designed. Conversely, there are several more possible forms of PYD-type EOS's due to the quadratic form in the denominator of Eq. 10; however, there are usually no degrees of freedom for these equations in designing the bonding and attractive terms to yield an overall cubic EOS. Finally, we could only find a single, yet interesting, NFQ-type model in the EOS literature.

The results presented in Tables 1 and 2 reveal some interesting insights. First, we note that all of the EOS's studied have the correct ideal gas limit of $Z_{HS}=1$ as $\eta\rightarrow 0$. However, 10 out of the 21 published equations listed have an incorrect limit of $g_{HS}(\sigma)\neq 1$ as $\eta\rightarrow 0$ and are, thus, thermodynamically incorrect according to our definition. Also, only two of the EOS models, van der Waals EOS[7] and Polishuk's vdWS1-type EOS[43] are only applicable to limited ranges of the isotropic fluid region ($\eta<0.495$), while an additional six of the models can be extended into the metastable liquid region ($0.495\leq\eta<0.740$), and another twelve models reach or exceed the solid face-centered-cubic (FCC) limit of $\eta=0.740$. Of note, is that the only model with a nearly exactly correct packing fraction pole of $\eta=0.740$ is Nasrifar and Bolland's PYD-type EOS.[48] This model is also thermodynamically correct and fairly accurate in the isotropic fluid region (i.e., 2.13 %AAD in Z_{HS} and 2.68 %AAD in $g_{HS}(\sigma)$ vs. η). The behavior of this EOS is compared to a similar new PYD-type model in Supporting Information Appendix A2 of this article.

Finally, the only NFQ-type equation found[51] has complex roots for η in the denominator in Eq. 10 and, thus, has no packing fraction pole. This EOS is also thermodynamically correct and highly accurate for $\eta<0.50$ (i.e., 0.47 %AAD in Z_{HS} and 0.82 %AAD in $g_{HS}(\sigma)$ vs. η). This EOS is compared

Table 1. Basic Forms and Attributes of Available Hard-Sphere Cubic Equation of State Components

Workers	EOS Type	Simplest Form of Z_{HS} Expression	Percent Deviation $g_{HS}(\sigma)$ at $\eta = 0$	η_{max}	Comments
van der Waals[7]	vdWS1	$Z_{HS} = \frac{1}{1-4\eta}$	0	0.250	Used in most empirical engineering cubic EOS's
Scott[34] Ishikawa et al.[35]	vdWS1	$Z_{HS} = \frac{1+2\eta}{1-2\eta}$	0	0.500	
Lin et al.[36] Kim et al.[37]	vdWS1	$Z_{HS} = \frac{1+3.08\eta}{1-1.68\eta}$	+19	0.595	Used in CCOR EOS
Elliott et al.[38]	vdWS1	$Z_{HS} = \frac{1+2.10\eta}{1-1.90\eta}$	0	0.525	Used in ESD EOS
Wang and Guo[39]	vdWS1	$Z_{HS} = \frac{1+2.6732\eta}{1-1.78976\eta}$	+12	0.559	
Mohsen-Nie et al.[40]	vdWS1	$Z_{HS} = \frac{1+2.48\eta}{1-1.88\eta}$	+9	0.532	
Chen et al.[41] Wang et al.[42]	vdWS1	$Z_{HS} = \frac{1+3.2804\eta}{1-1.6399\eta}$	+23	0.610	
Polishuk et al.[43]	vdWS1	$Z_{HS} = \frac{1+0.5\eta}{1-3.5\eta}$	0	0.286	
Nasrifar et al.[44]	vdWS1	$Z_{HS} = \frac{1+1.962\eta}{1-\eta}$	−26	1.000	
Dashtizadeh et al.[45]	vdWS1	$Z_{HS} = \frac{1+\eta}{1-\eta}$	−50	1.000	
Yelash et al.[46]	vdWS2	$Z_{HS} = 1 + \frac{4\eta+4.67\eta^2}{1-1.33\eta}$	0	0.752	Pole close to theoretical FCC solid limit $\eta_{max} = 0.741$
Thiele[9] Wertheim[1]	PYD	$Z_{HS} = 1 + \frac{4\eta+2\eta^2}{(1-\eta)^2}$	0	1.000	Theoretically-based Percus-Yevick EOS
Shah et al.[47]	PYD	$Z_{HS} = 1 + \frac{4.109\eta-1.655\eta^2}{(1-1.2865\eta)^2}$	+3	0.778	Pole close to theoretical FCC solid limit $\eta_{max} = 0.741$Repulsive term in empirical overall "quartic" EOS
Yelash et al.[46]	PYD	$Z_{HS} = 1 + \frac{4\eta+0.667\eta^2}{(1-\eta)(1-1.33\eta)}$	0	0.752	Pole very close to theoretical FCC solid limit $\eta_{max} = 0.741$
Nasrifar et al.[44]	PYD	$Z_{HS} = 1 + \frac{2.962\eta-0.4406\eta^2}{(1-\eta)^2}$	−26	1.000	
Nasrifar and Bolland[48]	PYD	$Z_{HS} = 1 + \frac{4\eta+0.596\eta^2}{(1-\eta)(1-1.351\eta)}$	0	0.740	Pole at theoretical FCC solid limit $\eta_{max} = 0.741$Thermodynamically Correct
Khanpour and Parsafar[49]	PYD	$Z_{HS} = 1 + \frac{4\eta-0.667\eta^2}{(1-1.33\eta)^2}$	0	0.752	Pole very close to theoretical FCC solid limit $\eta_{max} = 0.741$
Khanpour and Parsafar[49]	PYD	$Z_{HS} = 1 + \frac{3.96\eta-0.304\eta^2}{(1-1.205\eta)^2}$	+10	0.830	
Khanpour and Parsafar[49]	PYD	$Z_{HS} = 1 + \frac{3.841\eta+1.849\eta^2}{(1-1.107\eta)^2}$	−4	0.903	
Sun et al.[50]	PYD	$Z_{HS} = 1 + \frac{4\eta+1.192\eta^2}{(1-1.126\eta)^2}$	0	0.889	
De Lonngi and Villanueva[51]	NFQ	$Z_{HS} = 1 + \frac{4\eta-0.027152\eta^2}{(1-1.299\eta)^2+0.09\eta}$	0	NA	No pole (roots for η in denominator are complex)

with a similar new NFQ-type EOS presented in this article (Supporting Information Appendix A2).

In sum, we observe that there are a total of eight distinct functional forms in the EOS's reviewed. The set of eight new HS EOS's shown in Table 3 and evaluated in Table 4 were obtained by fitting Eq. 11 to molecular simulation data for $g_{HS}(\sigma)$ vs. η with various assumptions about the possible values of β_1 to β_3 and θ_2 (with $\theta_1 = 4$ in every case to ensure thermodynamic correctness). Table 3 lists our newly developed HS EOS's along with the "goodness of fit" (R^2 value) of $g_{HS}(\sigma)$ simulation data and the maximum packing fraction (η as $Z_{HS} \to \infty$).

Table 2. Parameters in Eq. 10 and Performance of Available Hard-Sphere Cubic Equation of State Components

Workers	EOS Type	β_1	β_2	β_3	θ_1	θ_2	$g_{HS}(\sigma)$ $\eta \to 0$	%AAD Z_{HS}	%AAD $g_{HS}(\sigma)$
van der Waals[7]	vdWS1	4	0	0	4	0	1	NA	NA
Scott[34] Ishikawa et al.[35]	vdWS1	2	0	0	4	0	1	149.33	164.11
Lin et al.[36] Kim et al.[37]	vdWS1	1.68	0	0	4.76	0	1.19	4.34	7.12
Elliott et al.[38]	vdWS1	1.90	0	0	4	0	1	27.04	31.42
Wang and Guo[39]	vdWS1	1.78976	0	0	4.46296	0	1.11574	10.73	12.95
Mohsen-Nie et al.[40]	vdWS1	1.88	0	0	4.36	0	1.09	24.35	27.5
Chen et al.[41] Wang et al.[42]	vdWS1	1.6399	0	0	4.9203	0	1.230075	3.38	6.81
Polishuk et al.[43]	vdWS1	3.5	0	0	4	0	1	NA	NA
Nasrifar et al.[44]	vdWS1	1	0	0	2.962	0	0.7405	37.44	53.73
Dashtizadeh et al.[45]	vdWS1	1	0	0	2	0	0.5	45.78	68.75
Yelash et al.[46]	vdWS2	1.33	0	0	4	4.67	1	7.54	9.41
Thiele[9] Wertheim[1]	PYD	1	1	0	4	2	1	5.25	6.52
Shah et al.[47]	PYD	1.2865	1.2865	0	4.109	−1.655	1.02725	2.04	2.79
Yelash et al.[46]	PYD	1	1.33	0	4	0.667	1	1.54	2.02
Nasrifar et al.[44]	PYD	1	1	0	2.962	−0.4406	0.7405	27.64	40.66
Nasrifar and Bolland[48]	PYD	1	1.351	0	4	0.596	1	2.13	2.68
Khanpour and Parsafar[49]	PYD	1.33	1.33	0	4	−0.667	1	8.17	9.57
Khanpour and Parsafar[49]	PYD	1.205	1.205	0	3.96	−0.304	0.99	2.02	3.32
Khanpour and Parsafar[49]	PYD	1.107	1.107	0	3.841	1.849	0.9603	0.91	1.91
Sun et al.[50]	PYD	1.126	1.126	0	4	1.192	1	0.31	0.6
De Lonngi and Villanueva[51]	NFQ	1.299	1.299	0.09	4	−0.027	1	0.47	0.82

New Hard-Sphere EOS Performance

This section assesses the ability of each of the eight new HS EOS's to describe Z vs. η behavior in the isotropic fluid and metastable liquid regions, isotropic fluid $g_{HS}(\sigma)$ vs. η, and the virial coefficient series up through B_{10}. Note that we will generally limit our analysis here to three representative equations (the most promising one each of the vdWS-, PYD-, and NFQ-type) due to the enormous task of trying to ultimately successfully compare all 21 new hard-sphere chain EOS's with each other, with existing models and with molecular simulation data. We provide comprehensive tables in Supporting Information, which parallel those given for the representative models in the main body of the text, containing the forms and statistical data for all eight hard-sphere equations and for the twenty-one hard-sphere chain EOS's that are produced from them. Graphical comparisons of representative published and new hard-sphere EOS performance vs. molecular simulation data are shown in Figures 2–4.

A comparison of isotropic fluid Z_{HS} vs. η from EOS models with molecular simulation data is given in Figure 2. The three representative new models, vdWS2-1, PYD-2, and NFQ-1 are in excellent agreement with simulation data (0.55, 1.17, and 0.58 %AAD, respectively). The two most popular repulsive terms in cubic and molecular-based EOS's, the CS EOS[10] (0.42 %AAD) and the original van der Waals EOS[7] (%AAD undetermined) are also shown for reference. The major conclusion from Figure 2, and an important contribution in this article, is that the proposed vdWS2-1, PYD-2, and NFQ-1 HS EOS's are accurate, thermodynamically correct cubic alternatives to the CS EOS. In fact, five of the eight new hard-sphere models in Table 2 have %AAD's considerably less than 1%.

The metastable fluid phase (high packing fraction) behavior of the above hard-sphere EOS's (excluding the van der Waals EOS with $Z^{HS} \to \infty$ at $\eta = 0.25$) is studied in Figure 3. Note that the relative errors with respect to simulation data are indeterminate for these cases because each of the EOS models considered has a pole (packing fraction value at which $Z^{HS} \to \infty$) considerably different than the theoretical (simulated) value of $\eta_{max} = 0.74$ for the FCC solid phase. The EOS's ranked in order of best-to-worst apparent performance are vdWS2-1, PYD-2, CS, and NFQ-1.

A significant finding, which is not directly apparent in the figure, is that the simulated Z_{HS} vs. η profile in the metastable liquid region eventually crosses the calculated profile for the vdWS2-1 EOS (pole at $\eta_{max} = 0.688$) at a value of Z_{HS} above where simulation data are available. The same behavior is not exhibited by the new PYD-2 EOS, which has a pole at $\eta_{max} = 0.837$. Perhaps the most interesting finding in Figure 3 is that the proposed NFQ-1 EOS has no packing fraction pole (i.e., the roots for η in the denominator of Eq. 10 are complex). Thus, the limit of this EOS's applicability is at about $\eta = 0.58$. Conversely, the CS EOS has a pole at unit packing fraction, considerably above the theoretical value of $\eta_{max} = 0.74$. Finally, the main conclusion from the plot is that the new vdWS2-1 EOS gives the best description of the metastable liquid region of all of the EOS's shown.

Table 3. Proposed HS EOS Components Determined from Fit of Molecular Simulation Data Including Goodness of Fit

EOS Acronym	Compressibility Factor Expression	$R^2 g_{HS}(\sigma)$	η_{max}
vdWS1-1	$Z_{HS} = \frac{1-2.283\eta}{1-1.717\eta}$	0.9488	0.582
vdWS2-1	$Z_{HS} = 1 + \frac{4\eta+5.3696\eta^2}{1-1.453\eta}$	0.9969	0.688
PYD-1	$Z_{HS} = 1 + \frac{4\eta}{(1-\eta)(1-1.372\eta)}$	0.9967	0.729
PYD-2	$Z_{HS} = 1 + \frac{4\eta}{(1-1.1942\eta)^2}$	0.9989	0.837
PYD-3	$Z_{HS} = 1 + \frac{4\eta+1.5072\eta^2}{(1-\eta)(1-1.211\eta)}$	0.9914	0.826
PYD-4	$Z_{HS} = 1 + \frac{4\eta+1.4068\eta^2}{(1-1.116\eta)^2}$	0.9895	0.896
NFQ-1	$Z_{HS} = 1 + \frac{4\eta}{1-2.5216\eta+1.7199\eta^2}$	0.9996	0.763
PYD-5	$Z_{HS} = 1 + \frac{4\eta+3\eta^2}{(1-0.5128\eta)(1-1.39285\eta)}$	0.9970	0.718

Table 4. Parameters in Eq. 10 and Performance of All Eight Proposed Hard-Sphere Cubic Equation of State Components

Acronym	β_1	β_2	β_3	θ_1	θ_2	$g_{HS}(\sigma)\ \eta \rightarrow 0$	%AAD Z_{HS}	%AAD $g_{HS}(\sigma)$
vdWS1-1	1.717	0	0	4	0	1	7.46	11.13
vdWS2-1	1.453	0	0	4	5.3696	1	0.55	0.86
PYD-1	1	1.372	0	4	0	1	1.63	2.45
PYD-2	1.1942	1.1942	0	4	0	1	1.17	1.93
PYD-3	1	1.211	0	4	1.5072	1	0.27	0.52
PYD-4	1.116	1.116	0	4	1.4068	1	0.28	0.53
NFQ-1	1.31145	1.31145	0.1013	4	0	1	0.58	0.94
PYD-5	0.51282	1.39285	0	4	3	1	0.34	0.56

Hard-sphere radial distribution function at contact value vs. packing fraction behavior in the isotropic liquid phase follows the same trend and ranking as compressibility factor; however, %AAD is always greater for $g_{HS}(\sigma)$ than for Z_{HS} vs. η. A comparison of the last two columns in Tables 2 and 4 verify this finding, which is not surprising as the compressibility factor and radial distribution function expressions are linked through Eq. 2 (the pressure equation). Moreover, several models in Table 2 fail to produce the correct ideal gas limit of $g_{HS}(\sigma) = 1$ as $\eta \rightarrow 0$. A graphical comparison of $g_{HS}(\sigma)$ vs. η for the same models studied in Figures 2 and 3 above is given in Supporting Information Appendix A1.

The final measure of hard sphere EOS performance investigated here is the virial coefficient series through the tenth virial coefficient predicted by the eight proposed HS EOS's. The nth virial coefficient for pure hard-spheres is defined as

$$B_n = \frac{1}{(n-1)!}\left(\frac{\partial^{n-1}Z}{\partial\eta^{n-1}}\right)_{\eta\rightarrow 0} \tag{18}$$

Recent molecular simulation data is available from Clisby and McCoy.[52] The Wolfram-Alpha derivative calculator was used to evaluate the derivatives in Eq. 18 for each of the models. Data and comparisons are given in Table 5 and Figure 4. First note that all of the new EOS terms have the correct theoretical value of the second-virial coefficient $B_2 = 4$ (i.e., requiring that $g_{HS}(\sigma) = 1$ as $\eta \rightarrow 0$ ensures that the theoretically correct value of B_2 is obtained). Plots of B_n vs. n (nth virial coefficient) for the selected proposed EOS models (vdWS2-1, PYD-2, and NFQ-1) are shown in Figure 4. The results of the plot are somewhat disappointing in the higher virial coefficient range ($n > 7$) for all three new models included. It is also noteworthy that B_n vs. n is above the theoretical values for the vdWS2-1 and PYD-2 models, whereas virial coefficients for the NFQ-1 EOS exhibit a maximum at B_9. While the results shown in Figure 4 are less than encouraging, a close inspection of Supporting Information Table A1–3 indicates that the new PYD-3 and PYD-4 EOS's nearly exactly reproduce theoretical values of the hard-sphere virial coefficients through B_{10}. Thus, these equations should be investigated further in future work. In summary, the entirety of the data in Tables 3 and 4 indicates that most of the eight new cubic HS EOS's proposed in this article are potential alternatives to the popular noncubic CS EOS. The number of possible tests and comparisons for all of these models is well beyond the scope of a single article.

Bonding and Dimer Compressibility Factor Contributions

Each of the eight newly developed HS EOS's (three representative models evaluated above) may be combined with a theoretical platform (i.e., TPT-D, HSC, or GFD) to obtain a chain fluid EOS. We require an expression for the bonding compressibility factor Z_{Bond}: $1 + \eta[\partial \ln g_{HS}(\sigma)/\partial\eta]$ in Eq. 3 for TPT-D, or a "cubic" equivalent expression for $g_{HS}^{PY}(\sigma)$ in Eq. 6 for HSC or for Z_{DB} in Eq. 7 for GFD. The bonding term for TPT-D is obtained by taking the indicated derivative. However, Z_{Bond} expressions for the HSC and GFD models are obtained by refitting either Chiew's[22] expression for $g_{HS}^{PY}(\sigma)$ vs. η or Tildesly and Streetts'[53] expression for Z_{DB} vs. η to identical polynomial forms in denominators of the corresponding Z_{HS} terms with numerators including powers up through η^2 (to give an overall cubic EOS).

Eight chain EOS's (two for TPT-D and three each for HSC and GFD) were obtained from the three representative models (vdWS2-1, PYD-2, and NFQ-1). The bonding compressibility factor expressions and goodness-of-fit measures for the three selected new hard-sphere EOS models (vdWS2-1, PYD-2, and NFQ-1) used in the three chain fluid theoretical platforms are given in Table 6. Z_{Bond} expressions were derived for the PYD-2 and NFQ-1 models, which retain the overall cubic form including the bonding contribution within the TPT-D framework. The errors are 1.85 and 1.35 %AAD for the PYD-2 and NFQ-1 HS EOS's, respectively, compared to Z_{Bond} vs. η derived from the CS EOS.

We report both "goodness of fit" (R^2 values) and relative error (%AAD) with respect to the original $g_{HS}^{PY}(\sigma)$[22] or Z_{DB}[53] expression for HSC and GFD (as original models were refit to cubic forms). The results for the HSC bonding compressibility factor expressions for the selected models range from 0.9859 to 0.9978 R^2 and from 0.20 to 1.03 %AAD, while the GFD bonding compressibility factor results span from 0.9992 to 0.9998 R^2 and from 0.30 to 0.50 %AAD. In all cases, the results of the fits are from very-good-to-excellent.

Z_{Bond} vs. η for PYD-2 and NFQ-1 within each of the TPT-D and HSC platforms is plotted in Figure 5. Z_{Bond} for the CS EOS (TPT-D) and Chiew's RDF (HSC) are denoted by the symbols. The bonding terms for the PYD-2 and NFQ-1 cubic TPT-D models are accurate to about $\eta = 0.35$ and 0.42, respectively. However, Z_{Bond} vs. η for PYD-2 and NFQ-1 in the HSC framework nearly exactly match Chiew's RDF to $\eta = 0.50$ (upper limit of liquid stability). These excellent results show that mathematically more complex bonding terms from original versions of HSC and GFD may be successfully repackaged in simpler "cubic" forms.

The TPT-D bonding framework requires additional information about the dimer fluid in the form of the hard-dimer radial distribution function at contact value $g_{HD}(\sigma)$. Both theoretical models[20,30,31,54] and simulation data[21] are available. Furthermore, empirical and theoretical relationships between $g_{HD}(\sigma)$ and $g_{HS}(\sigma)$ have been advanced. Sadus[55] proposed a linear relationship of the form

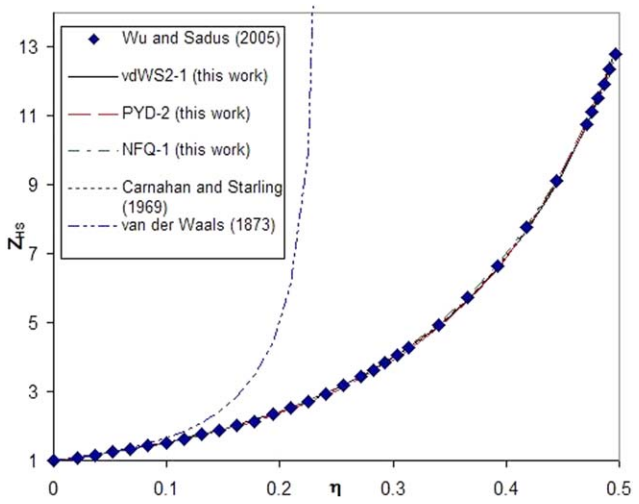

Figure 2. Calculated and simulated[57] isotropic fluid compressibility factor vs. packing fraction for hard-sphere equations of state.

[Color figure can be viewed in the online issue, which is available at wileyonlinelibrary.com.]

$$g_{HD}(\sigma)=g_{HS}(\sigma)(\alpha\eta+C) \tag{19}$$

Various authors have suggested values for the constants α and C in Eq. 19. Yethiraj and Hall[54] observed that $\alpha=0.42$ and $C=0.534$ from a fit of molecular simulation data for the hard-sphere and hard-dimer pair correlation functions. Sadus[55,56] proposed that $C=0.5$ and that $\alpha=0.7666$ or $\alpha=1.2313$ based on second-virial coefficient data for different EOS's. However, our fit of molecular simulation data for $g_{HD}(\sigma)$ and $g_{HS}(\sigma)$ gives results ($\alpha=0.4783$ and $C=0.5214$) closer to those of Yethiraj and Hall.[54] The goodness of fit of molecular simulation data is $R^2=0.9994$, which is excellent (see Supporting Information Figure A2–5).

A theoretical relationship between monomer and dimer pair correlation functions has been obtained by Nasrifar and Bolland[48] who quantified in terms of molecular surface areas of dimers and monomers the suggestion by Chang and Sandler[21] that the formation of tetramers from dimers is energetically less favorable than the formation of dimers from

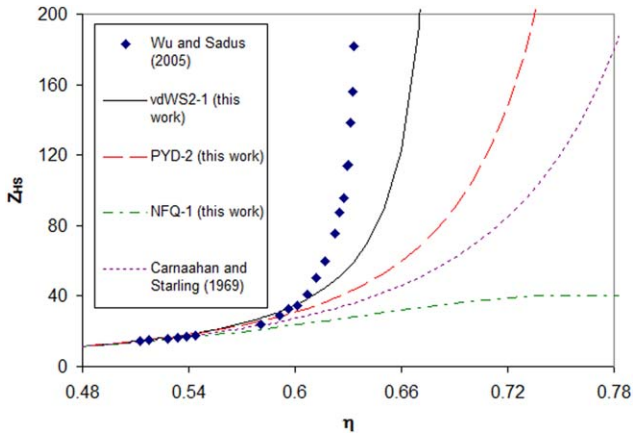

Figure 3. Calculated and simulated[57] metastable liquid compressibility factor vs. packing fraction for hard-sphere equations of state.

[Color figure can be viewed in the online issue, which is available at wileyonlinelibrary.com.]

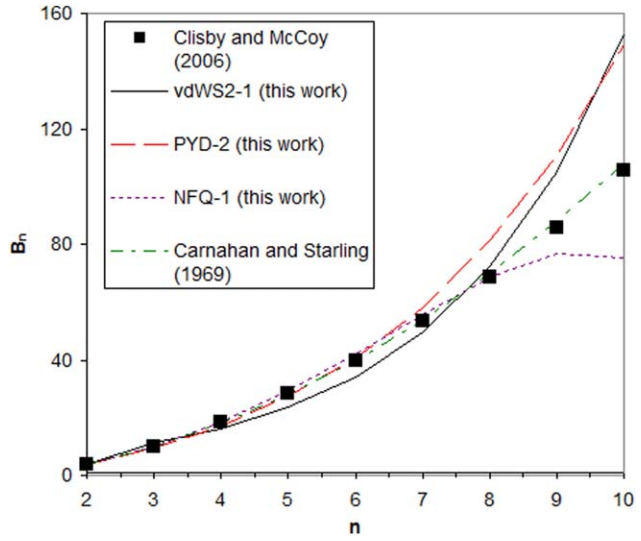

Figure 4. Comparison of hard sphere virial coefficient series for three new EOS models with Monte-Carlo integration data[52] (symbols in the figure).

[Color figure can be viewed in the online issue, which is available at wileyonlinelibrary.com.]

monomers. Ultimately, they showed using statistical mechanical arguments that

$$\ln g_{HD}(\sigma)=a\ \ln g_{HS}(\sigma)-b \tag{20}$$

where $a=1.260$ and $b=0.6931$. We have found that $a=1.2068$ and $b=0.6139$ using $g_{HS}(\sigma)$ and $g_{HD}(\sigma)$ simulation data of Wu and Sadus[57] and Chang and Sandler,[21] respectively. Our fit, shown in Figure 6, has R^2 of 0.9993.

The Sadus and Nasrifar and Bolland correlations (Eq. 19 with $\alpha=0.4783$ and $C=0.5214$ and Eq. 20 with $a=1.2068$ and $b=0.6139$, respectively) were applied to each of the $g_{HS}(\sigma)$ expressions obtained from Eq. 11 with parameter sets in Table 4 that produced a $g_{HD}(\sigma)$ expression consistent with an overall cubic EOS within the TPT-D framework (Eq. 3). Results for two representative models that meet this criterion (i.e., PYD-2NB and NFQ-1NB) are shown in Table 7 and Figure 7. Table 7 gives the analytical $g_{HD}(\sigma)$ expressions and the %AAD with respect to $g_{HD}(\sigma)$ molecular simulation data.[21] The errors are 0.94 and 3.53 %AAD for the NFQ-1NB and PYD-2NB models,

Table 5. Hard-Sphere Virial Coefficients for Selected New HS EOS Components Compared to Molecular Simulation Values and Values Calculated from the Carnahan-Starling EOS

	B_n				
n Model	MC	CS	vdWS2-1	PYD-2	NFQ-1
2	4	4	4	4	4
3	10	10	11.18	9.55	10.09
4	18.36	18	16.25	17.11	18.55
5	28.22	28	23.61	27.25	29.43
6	39.82	40	34.30	40.68	42.32
7	53.34	54	49.84	58.29	56.09
8	68.53	70	72.41	81.22	68.64
9	85.81	88	105.22	110.84	76.61
10	105.78	108	152.88	148.91	75.14
%AAD	0	1.24	14.76	12.74	6.39

Table 6. Bonding Compressibility Factor Contribution for Selected Proposed EOS Models Within the Three Theoretical Platforms

Hard-Sphere Model	Bonding Framework	Z_{Bond} Expression	R^2	%AAD
PYD-2	TPT1	$Z_{Bond}=1+\frac{2\beta_1\eta}{1-\beta_1\eta}$	NA	1.85
NFQ-1	TPT1	$Z_{Bond}=1+\frac{[2\beta_1(1-\beta_1\eta)-\beta_3]\eta}{(1-\beta_1\eta)^2+\beta_3\eta}$	NA	1.35
CS	TPT1	$Z_{Bond}=1+\frac{3\eta}{1-\eta}-\frac{\frac{1}{2}\eta}{1-\frac{1}{2}\eta}$	NA	0
vdWS2-1	HSC	$Z_{Bond}=\frac{1+1.3411\eta-0.992\eta^2}{1-1.453\eta}$	0.9859	1.03
PYD-2	HSC	$Z_{Bond}=\frac{1+0.2175\eta-1.1371\eta^2}{(1-1.1942\eta)^2}$	0.9940	0.39
NFQ-1	HSC	$Z_{Bond}=\frac{1-0.043\eta-0.5694\eta^2}{1-2.5216\eta+1.7199\eta^2}$	0.9978	0.20
Chiew	HSC	$Z_{Bond}=g_{HS}^{PY}(\sigma)=\frac{1+\frac{1}{2}\eta}{(1-\eta)^2}$	NA	0
vdWS2-1	GFD	$Z_{Bond}=\frac{1+3.6169\eta+13.574\eta^2}{1-1.453\eta}$	0.9998	0.50
PYD-2	GFD	$Z_{Bond}=\frac{1+3.5131\eta+3.7461\eta^2}{(1-1.1942\eta)^2}$	0.9992	0.92
NFQ-1	GFD	$Z_{Bond}=\frac{1+2.9168\eta+5.0528\eta^2}{1-2.5216\eta+1.7199\eta^2}$	0.9998	0.30
Tildesley-Streett	GFD	$Z_{Bond}=\frac{1+2.45696\eta+4.10386\eta^2-3.75503\eta^3}{(1-\eta)^3}$	NA	0

respectively. Table 7 and Figure 7 also show that there is a 4.31% discrepancy between the widely accepted Chiew integral equation theory $g_{HD}(\sigma)$ expression and the molecular simulation data of Chang and Sandler[21] leaving an unresolved issue regarding which hard-dimer pair correlation function at contact value is more suitable, the simulated or theoretical function? Evidence given in the next section of this article suggests that Chiew's theoretical $g_{HD}(\sigma)$ expression gives better results for chain fluid compressibility factor vs. packing fraction.

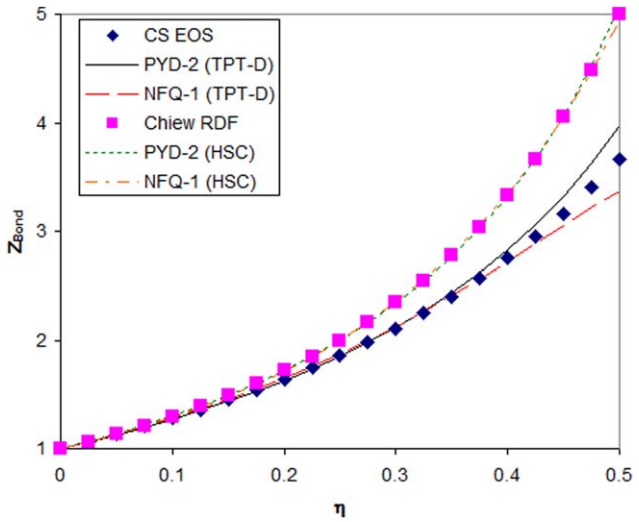

Figure 5. Bonding compressibility factor vs. packing fraction for selected HS EOS models using the TPT and HSC platforms.

[Color figure can be viewed in the online issue, which is available at wileyonlinelibrary.com.]

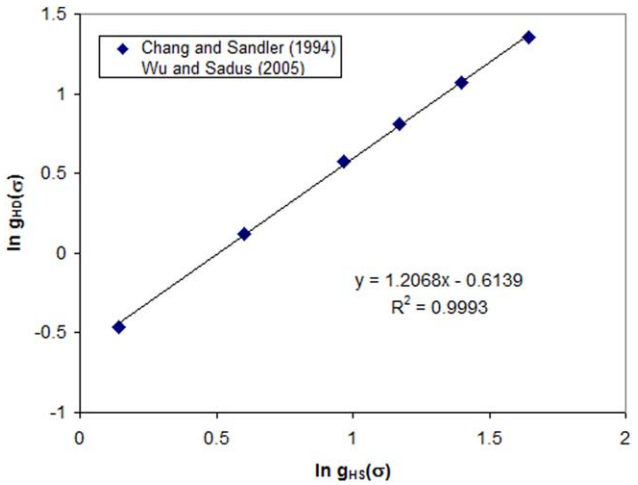

Figure 6. Observed linear relationship between ln $g_{HD}(\sigma)$ and ln $g_{HS}(\sigma)$.

The points were determined from molecular simulation data for $g_{HD}(\sigma)$[21] and $g_{HS}(\sigma)$[57] available at the same packing fraction. [Color figure can be viewed in the online issue, which is available at wileyonlinelibrary.com.]

Table 7. Dimer Compressibility Factor Contribution for Selected TPT-D Models

Hard Sphere Model	Hard Dimer Framework	Z_{Dimer} Expression	%AAD $g_{HD}(\sigma)$
Chiew (1991)	NA	$Z_{Dimer}=\frac{\frac{1}{2}+\eta}{(1-\eta)^2}$	4.31
PYD-2	Nasrifar and Bolland (2006)	$Z_{Dimer}=1+\frac{2.4136\beta_1\eta}{1-\beta_1\eta}$	3.53
NFQ-1	Nasrifar and Bolland (2006)	$Z_{Dimer}=1+\frac{1.2068[2\beta_1(1-\beta_1\eta)-\beta_3]\eta}{(1-\beta_1\eta)^2+\beta_3\eta}$	0.94

Chain Pure Fluid and Mixture EOS Performance

The 21 chain EOS's in the three theoretical platforms were tested for predictive ability for Z^m vs. η for homonuclear athermal chains. The complete analytical forms of Z^m vs. η and P vs. V for the 21 new chain EOS's are presented in Supporting Information Tables A2–5a and b. We consider here only the eight EOS models obtained using vdWS2-1, PYD-2, and NFQ-1 within each of the TPT-D, HSC, and GFD platforms (Tables 8 and 9). The molar volume V is related to packing fraction by $\eta = c/V$ where c is a parameter related to the number of segments and the segment size (see Eq. 5). Molecular simulation data[32] are available for chains ranging from $m = 2$ to $m = 201$ homonuclear segments. Table 10 gives errors in Z^m vs. η with respect to simulation data.

Some trends in the data are apparent. The average errors generally increase for all models as chain length increases. Furthermore, original TPT-D1 (3.15 %AAD overall) does modestly better than its cubic counterparts PYD-2NBTPT and NFQ-1NBTPT (4.26 and 3.82 %AAD overall, respectively). In contrast, and somewhat unexpectedly (as the cubic models are a repackaging of more complex original forms), two of the three cubic chain EOS models outperform their original noncubic counterparts in each of the other two platforms. vdWS2-1HSC and NFQ-1HSC (6.11 and 6.14 %AAD overall, respectively) are marginally superior to the original PY-Chiew HSC model (6.61 %AAD overall). Similarly, vdWS2-1GFD and NFQ-1GFD (3.94 and 3.81 %AAD overall, respectively) are clearly better than the original GFD model (4.51 %AAD overall).

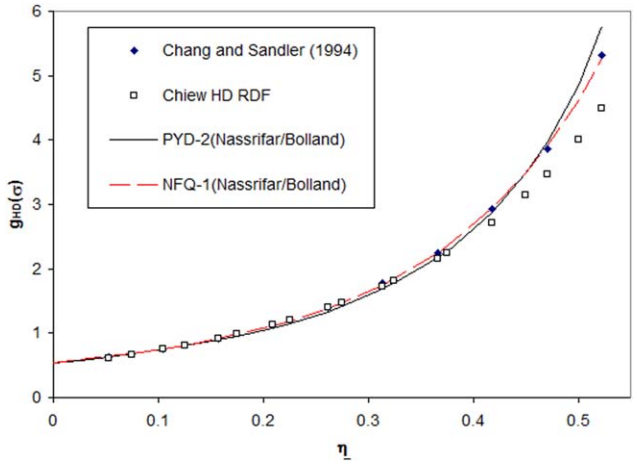

Figure 7. Hard-dimer radial distribution function vs. packing fraction in TPT-D framework for two new HS EOS bonding terms used with the Nasrifar–Bolland correlation.

[Color figure can be viewed in the online issue, which is available at wileyonlinelibrary.com.]

A comparison of EOS performance is given in Figure 8 for chains with 201 segments ($m = 201$). The plot compares the new cubic models within the NBTPT-D framework, PYD-2NBTPT, and NFQ-1NBTPT, to the original TPT-D1 model [based on the CS EOS and Chiew's expression for $g_{HD}(\sigma)$]. A cursory glance at the errors in Table 10 (8.24, 7.22, and 5.89 %AAD for PYD-2NBTPT, NFQ-1NBTPT, and TPT-D1, respectively) suggests that the original TPT-D model is definitively more accurate for long chain fluids. However, the data in Figure 8 clearly show that PYD-2NBTPT does better at higher density.

The 21 new EOS models were also tested for their ability to predict second-virial coefficient of pure chain fluids. The reduced second-virial coefficient $B_2/m^2\sigma^3$ is given by[56]

$$\frac{B_2}{m^2\sigma^3}=\frac{\pi}{6m}\left(\frac{\partial Z_m}{\partial\eta}\right)_{\eta\to 0} \tag{21}$$

Equations 3, 6, and 7 may be rewritten as

$$Z^m=a_0Z_{HS}+a_1Z_{Bond}+a_2Z_{Dimer} \tag{22}$$

where $a_0 = m$, $a_1 = -m/2$ and $a_2 = -(m/2 - 1)$ for TPT-D; $a_0 = m$, $a_1 = -(m - 1)$ and $a_2 = 0$ for HSC; and $a_0 = -Y^m$, $a_1 = Y^m + 1$ and $a_2 = 0$ for GFD. Differentiation of Eq. 22 with respect to packing fraction and evaluation as $\eta \to 0$ yields

$$\left(\frac{\partial Z^m}{\partial\eta}\right)_{\eta\to 0}=a_0\left(\frac{\partial Z_{HS}}{\partial\eta}\right)_{\eta\to 0}+a_1\left(\frac{\partial Z_{Bond}}{\partial\eta}\right)_{\eta\to 0}+a_2\left(\frac{\partial Z_{Dimer}}{\partial\eta}\right)_{\eta\to 0} \tag{23}$$

as the general form of the derivative in Eq. 23. First, note that the hard-sphere contribution $(\partial Z_{HS}/\partial\eta)_{\eta\to 0}$ is identically 4 for all EOS's in all three theories (see Table 5). Table 11 gives the values of $(\partial Z_{Bond}/\partial\eta)_{\eta\to 0}$ and $(\partial Z_{Dimer}/\partial\eta)_{\eta\to 0}$ for Eq. 23, which is combined with Eq. 21 to determine the reduced second-virial coefficient $B_2/m^2\sigma^3$ vs. m for all eight representative new cubic EOS's and the original model in each platform. Errors with respect to simulation data are also listed (Supporting Information Table A2–7 presents this information for all 21 new cubic EOS's). Errors in all models, including the original noncubic equations in each platform, are quite high (in excess of 10 %AAD). Figure 9 shows the reduced second-virial coefficient $B_2/m^2\sigma^3$ vs. segment number m for the vdWS1-1HSC (15.14 %AAD from Supporting Information Table A2–7) and vdWS2-1HSC (37.36 %AAD) vs. the original HSC model with an error of 61.53 %.

The bonding and dimer contributions in Table 11 provide insight as to where improvements can be made. Thus, better results are only possible by improving the dimer term to obtain a higher value of $(\partial Z_{Dimer}/\partial\eta)_{\eta\to 0}$ assuming TPT-D

Table 8. Complete Packing Factor Forms of Selected New Athermal Hard-Sphere Chain Equations of State

EOS	Z^m Expression
PYD-2NBTPT	$Z^m = m\left[1+\frac{4\eta}{(1-1.1942\eta)^2}\right]-\frac{m}{2}\left(1+\frac{2.3884\eta}{1-1.1942\eta}\right)-\left(\frac{m}{2}-1\right)\left(1+\frac{2.8823\eta}{1-1.1942\eta}\right)$
NFQ-1NBTPT	$Z^m = m\left(1+\frac{4\eta}{1-2.5216\eta+1.7199\eta^2}\right)-\frac{m}{2}\left(1+\frac{2.5216\eta-3.4398\eta^2}{1-2.5216\eta+1.7199\eta^2}\right)-\left(\frac{m}{2}-1\right)\left(1+\frac{3.0431\eta-4.1512\eta^2}{1-2.5216\eta+1.7199\eta^2}\right)$
vdWS2-1HSC	$Z^m = m\left(1+\frac{4\eta+5.3696\eta^2}{1-1.453\eta}\right)-(m-1)\left(\frac{1+1.3411\eta-0.992\eta^2}{1-1.453\eta}\right)$
PYD-2HSC	$Z^m = m\left[1+\frac{4\eta}{(1-1.1942\eta)^2}\right]-(m-1)\left[\frac{1+0.2175\eta-1.1371\eta^2}{(1-1.1942\eta)^2}\right]$
NFQ-1HSC	$Z^m = m\left(1+\frac{4\eta}{1-2.5216\eta+1.7199\eta^2}\right)-(m-1)\left(\frac{1-0.043\eta-0.5694\eta^2}{1-2.5216\eta+1.7199\eta^2}\right)$
vdWS2-1GFD	$Z^m = -Y^m\left(1+\frac{4\eta+5.3696\eta^2}{1-1.453\eta}\right)+(Y^m+1)\left(\frac{1+3.6169\eta+13.574\eta^2}{1-1.453\eta}\right)$
PYD-2GFD	$Z^m = -Y^m\left[1+\frac{4\eta}{(1-1.1942\eta)^2}\right]+(Y^m+1)\left[\frac{1+3.5131\eta+3.7461\eta^2}{(1-1.1942\eta)^2}\right]$
NFQ-1GFD	$Z^m = -Y^m\left(1+\frac{4\eta}{1-2.5216\eta+1.7199\eta^2}\right)+(Y^m+1)\left(\frac{1-0.043\eta-0.5694\eta^2}{1-2.5216\eta+1.7199\eta^2}\right)$

to be an accurate and theoretically correct platform. Moreover, the data suggest that $(\partial Z_{\text{Bond}}/\partial\eta)_{\eta\to 0}$ should be higher than the value for the original HSC model and lower than the value for the original GFD model. Clearly, more work is needed in this area to resolve these issues.

Finally, other more accurate bonding platforms may be considered. For instance, TPT-D assumes that molecules are composed of homonuclear tangent spherical segments. Clearly, this is an approximation that can be relaxed by assuming the existence of heteronuclear overlapping

Table 9. Pressure Explicit Forms of Selected New Athermal Hard-Sphere Chain Equations of State

EOS	Z^m Expression
PYD-2NBTPT	$P = m\left[\frac{RT}{V}+\frac{4cRT}{(V-1.1942c)^2}\right]-\frac{m}{2}\left[\frac{RT}{V}+\frac{2.3884cRT}{V(V-1.1942c)}\right]-\left(\frac{m}{2}-1\right)\left[\frac{RT}{V}+\frac{2.8823cRT}{V(V-1.1942c)}\right]$
NFQ-1NBTPT	$P = m\left[\frac{RT}{V}+\frac{4cRT}{V^2-2.5216cV+1.7199c^2}\right]-\frac{m}{2}\left[\frac{RT}{V}+\frac{(2.5216cV-3.4398c^2)RT}{V(V^2-2.5216cV-1.7199c^2)}\right]-\left(\frac{m}{2}-1\right)\left[\frac{RT}{V}+\frac{(3.0431cV-4.1512c^2)RT}{V(V^2-2.5216cV-1.7199c^2)}\right]$
vdWS2-1HSC	$P = m\left[\frac{RT}{V}+\frac{(4cV+5.3696c^2)RT}{V^2(V-1.453c)}\right]-(m-1)\left[\frac{(V^2+1.3411cV-0.992c^2)RT}{V^2(V-1.453c)}\right]$
PYD-2HSC	$P = m\left[\frac{RT}{V}+\frac{4cRT}{(V-1.1942c)^2}\right]-(m-1)\left[\frac{(V^2+0.2175cV-1.1371c^2)RT}{V(V-1.1942c)^2}\right]$
NFQ-1HSC	$P = m\left[\frac{RT}{V}+\frac{4cRT}{V^2-2.5216cV+1.7199c^2}\right]-(m-1)\left[\frac{(V^2-0.043cV-0.5694c^2)RT}{V(V^2-2.5216cV+1.7199c^2)}\right]$
vdWS2-1GFD	$P = -Y^m\left[\frac{RT}{V}+\frac{(4cV+5.3696c^2)RT}{V^2(V-1.453c)}\right]+(Y^m+1)\left[\frac{(V^2+3.6169cV+13.574c^2}{V^2(V-1.453c)}\right]$
PYD-2GFD	$P = -Y^m\left[\frac{RT}{V}+\frac{4cRT}{(V-1.1942c)^2}\right]+(Y^m+1)\left[\frac{(V^2+3.5131cV+3.7461c^2)RT}{V(V-1.1942c)^2}\right]$
NFQ-1GFD	$P = -Y^m\left[\frac{RT}{V}+\frac{4cRT}{V^2-2.5216cV+1.7199c^2}\right]+(Y^m+1)\left[\frac{(V^2-0.043cV-0.5694c^2)RT}{V(V^2-2.5216cV+1.7199c^2)}\right]$

Table 10. Summary of Errors in Z^m vs. η for Selected New Cubic Equations of State and Noncubic Reference EOS's

M	2	3	4	8	16	32	51	201	All
# of Points	5	5	18	7	17	4	9	8	73
Model					%AAD				
PYD-2NBTPT	2.18	1.81	2.42	5.46	4.28	5.64	5.36	8.24	4.26
NFQ-1NBTPT	0.70	1.70	2.69	4.38	4.19	6.24	3.76	7.22	3.82
vdWS2-1HSC	4.23	4.47	4.97	5.89	5.41	6.26	7.72	10.67	6.11
PYD-2HSC	5.24	5.10	6.63	7.59	5.68	7.28	8.56	11.27	7.08
NFQ-1HSC	3.61	3.30	4.02	6.63	6.03	7.63	7.97	11.26	6.14
vdWS2-1GFD	1.13	1.36	2.40	5.58	4.68	6.24	3.81	6.72	3.94
PYD-2GFD	1.72	1.69	2.73	10.48	10.05	14.10	8.73	12.94	7.52
NFQ-1GFD	0.88	1.04	2.08	5.44	4.15	5.78	4.46	7.41	3.81
TPT-D1	1.03	1.97	2.40	2.88	3.74	4.18	2.71	5.89	3.15
PY-Chiew	4.33	4.10	5.19	7.13	5.91	7.59	8.36	11.39	6.61
GFD	0.99	0.76	2.37	6.64	5.38	7.92	4.81	8.12	4.51

segments (e.g., an *n*-alkane is composed of different-sized soft or Lennard-Jones spherical segments).

We briefly consider application of the eight selected proposed EOS chain models to AHSC mixtures. Simulation data are available[58] for homonuclear dimer (1)–tetramer (2) mixtures. Supporting Information Appendix A3 examines some cases where the segments in each species differ in size. Assuming that mixing occurs at constant total volume, we have that

$$m = x_1 m_1 + x_2 m_2 \tag{24}$$

where x_i is the mole fraction of component i. The origin of Eq. 24 can clearly be seen in the derivation in Supporting Information Appendix A3. Results including relative errors for the eleven (eight new and three original) representative chain mixture models in this article using Eq. 24 for m are presented in Table 12, and an illustration is given in Figure 10.

The general ranking of the bonding framework appears to be GFD (best), TPT-D (intermediate), and HSC (worst). Specifically, the vdWS2-1 EOS is better than the original models within both the HSC and GFD platforms (4.49 and 0.38 vs. 5.25 and 0.70 %AAD for cubic vs. HSC and GFD original models, respectively). Similarly, the NFQ-1 EOS is superior to the original models within both TPT-D and HSC (1.16 and 3.92 vs. 1.24 and 5.25 %AAD for cubic vs. TPT-D and HSC original models, respectively). Not surprisingly, these results parallel those in Table 10 for pure fluids.

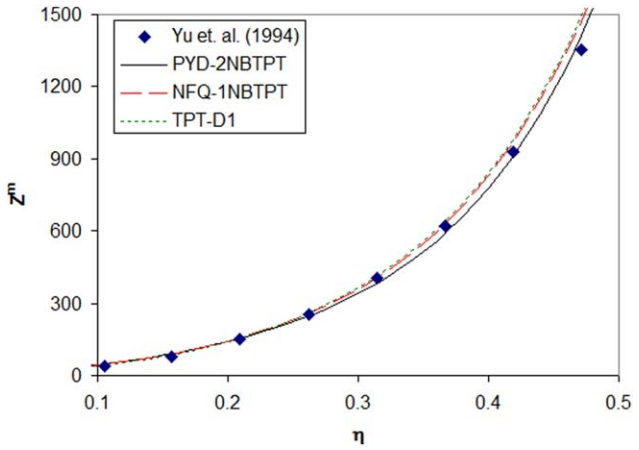

Figure 8. Predicted (TPT-D models) and simulated compressibility factor vs. packing fraction for hard sphere chains consisting of 201 segments ($m = 201$).

[Color figure can be viewed in the online issue, which is available at wileyonlinelibrary.com.]

Figure 10 compares vdWS2-1HSC and vdWS2-1GFD with each other, the respective original noncubic models and simulation data for equimolar binary dimer-tetramer mixtures. Profiles for both vdWS2-1GFD and the corresponding original GFD model agree very well with simulation data,[58] whereas vdWS2-1HSC and CS-PY both underpredict the simulated Z^m vs. η data to about the same degree, and the trend becomes more pronounced as packing fraction increases.

Conclusions

A universal form for the hard-sphere EOS, identified from a review of the EOS literature, was used to develop eight new thermodynamically correct HS EOSs. These equations were incorporated into three theoretical platforms (TPT-D, HSC, and GFD) to develop 21 new cubic EOS's for athermal chain fluids (five for TPT-D and eight each for HSC and GFD). Features of this approach include two new relationships between $g_{HD}(\sigma)$ and $g_{HS}(\sigma)$ in TPT-D and empirically refit forms of bonding terms in HSC and GFD.

Tests and comparisons of the 21 new cubic EOS's were made (results for a representative set of eight models, two for TPT-D and three each for HSC and GFD were presented). The eight hard-sphere models were assessed for ability to represent molecular simulation data for

Table 11. Second-Virial Coefficient Contributions in Eqs. 36–38 and Errors in Reduced Second-Virial Coefficient $B_2/m^2\sigma^3$ vs. m for Selected TPT-D, HSC, and GFD Models, Respectively

EOS Model	$\left(\frac{\partial Z_{HS}}{\partial \eta}\right)_{\eta\to 0}$	$\left(\frac{\partial Z_{Bond}}{\partial \eta}\right)_{\eta\to 0}$	$\left(\frac{\partial Z_{Dimer}}{\partial \eta}\right)_{\eta\to 0}$	%AAD
PYD-2NBTPT	4	2.3884	2.8823	51.88
NFQ-1NBTPT	4	2.5216	3.0431	39.34
TPT-D1	4	2.5	4	10.07
vdWS2-1HSC	4	2.7941	NA	37.36
PYD-2HSC	4	2.6059	NA	52.57
NFQ-1HSC	4	2.4786	NA	63.64
CS-PY	4	2.5	NA	61.53
vdWS2-1GFD	4	5.0699	NA	26.36
PYD-2GFD	4	5.9015	NA	92.82
NFQ-1GFD	4	5.4384	NA	53.78
GFD	4	5.4570	NA	55.32

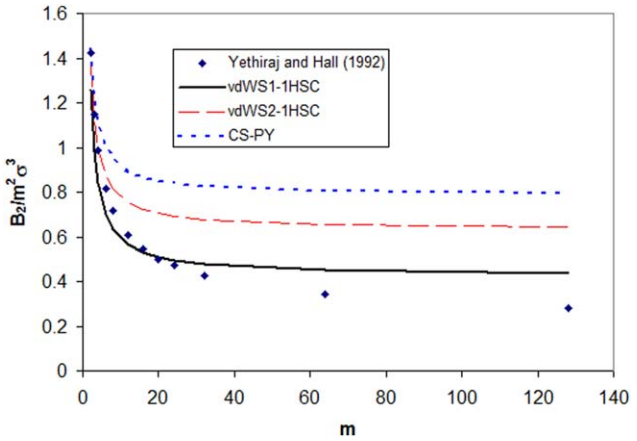

Figure 9. Reduced second-virial coefficient $B_2/m^2\sigma^3$ vs. m for two vdWS-HSC models compared to molecular simulation data.[31]

[Color figure can be viewed in the online issue, which is available at wileyonlinelibrary.com.]

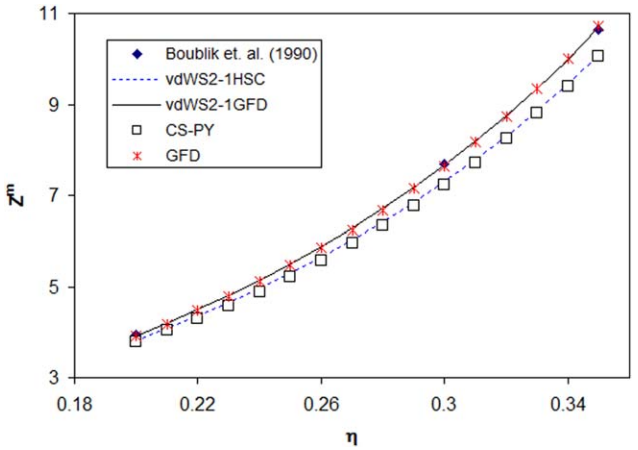

Figure 10. Predicted (HSC and GFD models) and simulated compressibility factor vs. packing fraction for equimolar binary dimer-tetramer mixtures.

[Color figure can be viewed in the online issue, which is available at wileyonlinelibrary.com.]

compressibility factor and radial distribution function vs. packing fraction. Several models including vdWS2-1, PYD-2, and NFQ-1 appear to be potential substitutes for the widely used noncubic CS EOS. The virial coefficient series up through B_{10} was also calculated for each of the three representative models and compared with theoretical values.

The 21 new HS chain EOS's were tested for their ability to predict properties for hard-sphere chain pure fluids and mixtures. Results (for representative EOS's) suggested that the original TPT-D1 model and the new vdWS2-1 and NFQ-1 HS EOS's in both the HSC and GFD platforms are the best models for Z^m vs. η. Moreover, none of the new or published chain fluid models was able to adequately predict reduced second-virial coefficient $B_2/m^2\sigma^3$ vs. segment number m (errors in excess of 10 %AAD). Finally, the eight representative EOS models were used to successfully predict Z^m vs. η for a homonuclear binary mixture.

Several of the 21 new models are sound candidates for the repulsive plus bonding backbone in molecularly constructed cubic EOS's for "real" fluids. We are currently working on a parallel approach for deriving theoretically based compatible compressibility factor expressions for attractive effects that can be combined with the hard-sphere chain EOS's presented here to obtain cubic EOS's for real fluids of industrial interest.

Table 12. Errors for Binary Mixtures of Homonuclear Chains: Performance of Eight Selected New EOS Models vs. Molecular Simulation Data and Conventional Published Models

Model Mixture	Dimer(1)-Tetramer(2) $x_1 = x_2 = 0.50$ (three points) %AAD
PYD-2NBTPT	3.18
NFQ-1NBTPT	1.16
vdWS2-1HSC	4.49
PYD-2HSC	7.25
NFQ-1HSC	3.92
vdWS2-1GFD	0.38
PYD-2GFD	0.77
NFQ-1GFD	1.10
TPT-D1	1.24
CS-PY	5.25
GFD	0.70

Acknowledgments

The authors would like to thank both reviewers for many useful suggestions that significantly improved the quality of the article. The authors are also grateful to Professor Angelo Lucia, Department of Chemical Engineering, University of Rhode Island for pre-reviewing the manuscript prior to its original submission. Finally, Evelina Woodruff, Library Technical Assistant at the University of New Haven was very helpful in obtaining several reference items through Interlibrary Loan.

Literature Cited

1. Wertheim MS. Exact solution of the Percus-Yevick integral equation theory for hard spheres. *Phys Rev Lett*. 1963;10:321–323.
2. Henderson D, Leonard PJ. One- and two-fluid van der Waals theories of liquid mixtures, 1. Hard-sphere mixtures. *Proc Natl Acad Sci*. 1970;67:1818–1823.
3. Barker JA, Henderson D. Theories of liquids. *Ann Rev Phys Chem*. 1972;23:439–484.
4. Hansen JP, McDonald IR. *Theory of Simple Liquids*. London: Academic Press, 1986.
5. Mulero A, editor. *Theory and Simulation of Hard-Sphere Fluids and Related Systems. Lecture Notes in Physics*, Vol. 753. Berlin, Heidelberg: Springer, 2008.
6. Gray CG, Gubbins KE, Joslin CJ, editors. *Theories of Molecular Fluids*, 2nd ed. Oxford: Oxford University Press, 2011.
7. van der Waals JD. *Over de Continuiteit van den Gas- en Vloeistoftoestand (On the Continuity of the Gas and Liquid State)*. Ph.D. Thesis. Leiden, The Netherlands: A. J. Sijthoff, 1873.
8. Redlich O, Kwong JNS. On the thermodynamics of solutions. V. An equation of state. Fugacities of gaseous solutions. *Chem Rev*. 1949; 44:233–244.
9. Theile E. Equation of state for hard spheres. *J Chem Phys*. 1963;39: 474–479.
10. Carnahan NF, Starling KE. Equation of state for non-attracting rigid spheres. *J Chem Phys*. 1969;51:635–636.
11. Soave G. Equilibrium constants from a modified Redlich-Kwong equation of state. *Chem Eng Sci*. 1972;27:1197–1203.
12. Peng D-Y, Robinson DB. A new two-constant equation of state. *Ind Eng Chem*. 1976;15:59–64.
13. Wei YS, Sadus RJ. Equations of state for the calculation of fluid phase equilibria. *AIChE J*. 2000;46:169–196.
14. Weeks JD, Chandler D, Andersen HC. Role of repulsive forces in determining the equilibrium structure of simple liquids. *J Chem Phys*. 1971;54:5237–5247.

15. Deiters U. A new semiempirical equation of state for fluids – I: derivation. *Chem Eng Sci*. 1981;36:1139–1146.
16. Chandler D, Weeks JD, Andersen HC. van der Waals picture of liquids, solids and phase transformations. *Science*. 1983;220:787–794.
17. Song Y, Mason EA. Statistical mechanical basis for accurate analytical equations of state for fluids. *Fluid Phase Equilib*. 1992;75:105–115.
18. Song Y, Lambert SM, Prausnitz JM. A perturbed hard-sphere-chain equation of state for normal fluids and polymers. *Ind Eng Chem Res*. 1994;33:1047–1057.
19. Mueller EA, Gubbins KE. Molecular-based equations of state for associating fluids: a review of SAFT and related approaches. *Ind Eng Chem Res*. 2001;40:2193–2211.
20. Ghonasgi D, Chapman WG. A new equation of state for hard-chain molecules. *J Chem Phys*. 1994;100:6633–6639.
21. Chang J, Sandler SI. An equation of state for the hard-sphere chain fluid: theory and Monte Carlo simulation. *Chem Eng Sci*. 1994;49:2777–2791.
22. Chiew YC. Percus-Yevick integral equation theory for athermal hard-sphere chains. Part I: equations of state. *Mol Phys*. 1990;70:129–143.
23. Song Y, Lambert SM, Prausnitz JM. Equation of state for mixtures of hard-sphere chains including copolymers. *Macromolecules*. 1994;27:441–448.
24. Dickman R, Hall CK. Equation of state for chain molecules: continuous-space analog of Flory theory. *J Chem Phys*. 1986;85:4108–4115.
25. Honnell KG, Hall CK. A new equation of state for athermal chains. *J Chem Phys*. 1989;90:1841–1855.
26. Wertheim MS. Fluids with highly directional attractive forces I. Statistical thermodynamics. *J Stat Phys*. 1984;35:19–34.
27. Wertheim MS. Fluids with highly directional attractive forces IV. Equilibrium polymerization. *J Stat Phys*. 1986;42:477–492.
28. Chapman WG, Jackson G, Gubbins KE. Phase equilibria of associating fluids. Chain molecules with multiple bonding sites. *Mol Phys*. 1988;65:1057–1079.
29. Huang SH, Radosz M. Equation of state for small, large, polydisperse and associating molecules. *Ind Eng Chem Res*. 1990;29:2284–2294.
30. Chiew YC. Percus-Yevick integral equation theory for athermal hard-sphere chains. II. Average intermolecular correlation functions. *Mol Phys*. 1991;73:359–373.
31. Yethiraj A, Hall CK. Monte Carlo simulations and integral equation theory for microscopic correlations in polymeric fluids. *J Chem Phys*. 1992;96:797–809.
32. Yu Y-X, Lu J-F, Tong J-S, Li Y-G. Equation of state for hard-sphere chain molecules. *Fluid Phase Equilib*. 1994;102:159–172.
33. Gulati HS, Hall CK. Generalized Flory equations of state for copolymers modeled as square-well chain fluids. *J Chem Phys*. 1998;108:7478–7492.
34. Scott RL. *Physical Chemistry: An Advanced Treatise, Vol. 8A, Chapter 1*. In: Eyring H, Henderson D, Wilhelm J, editors. New York: Academic Press, 1971.
35. Ishikawa T, Chung WK, Lu BCY. A cubic perturbed hard sphere equation of state for thermodynamic properties and vapor-liquid equilibrium calculations. *AIChE J*. 1980;26:372–378.
36. Lin HM, Kim H, Guo TM, Chao KC. Cubic chain-of-rotators equation of state and VLE calculations. *Fluid Phase Equilib*. 1983;13:143–152.
37. Kim H, Lin HM, Chao KC. Cubic chain-of-rotators equation of state. *Ind Eng Chem Fundam*. 1986;25:75–84.
38. Elliott JR, Suresh SJ, Donohue MD. A simple equation of state for nonspherical and associating molecules. *Ind Eng Chem Res*. 1990;29:1476–1484.
39. Wang LS, Guo TM. A cubic simplified perturbed hard-chain equation of state for fluids with chainlike molecules. *Can J Chem Eng*. 1993;71:591–604.
40. Mohsen-Nie M, Moddaress H, Mansoori GA. A simple cubic equation of state for hydrocarbons and other compounds. *68th Annual Technical Conference and Exhibition of the Society of Petroleum Engineers*. (Paper # SPE26667). Houston, TX, October 3–8, 1993.
41. Chen SF, Chow YL, Chen Y-P. A new simplified hard-body equation of state. *Fluid Phase Equilib*. 1996;118:201–219.
42. Wang H-T, Tsai J-C, Chen Y-P. A cubic equation of state for vapor-liquid equilibrium calculations of nonpolar and polar fluids. *Fluid Phase Equilib*. 1997;138:43–59.
43. Polishuk I, Wisniak J, Segura H. A novel approach for defining parameters in a four-parameter EOS. *Chem Eng Sci*. 2000;55:5855–5870.
44. Nasrifar K, Ayatollahi S, Moshfeghian M. Improving the simplified-perturbed-hard-chain theory equation of state using a new non-attracting hard-sphere equation. *Can J Chem Eng*. 2000;78:1111–1119.
45. Dashtizadeh A, Puzuki GR, Taghikhani V, Ghotbi G. A new cubic equation of state for predicting phase behavior of hydrocarbons. *Oil Gas Technol Rev IFP*. 2006;61:269–276.
46. Yelash LV, Kraska T, Deiters UK. Closed-loop critical curves in simple hard-sphere van der Waals-fluid models consistent with the packing fraction limit. *J Chem Phys*. 1999;110:3079–3084.
47. Shah VM, Bienkowski PR, Cochran HD. Generalized quartic equation of state for pure nonpolar fluids. *AIChE J*. 1994;40:152–159.
48. Nasrifar K, Bolland O. Simplified hard-sphere chain equations of state for engineering applications. *Chem Eng Commun*. 2006;193:1277–1293.
49. Khanpour M, Parsafar GA. A simple method of generating equations of state for hard sphere fluid. *Chem Phys*. 2007;333:208–213.
50. Sun J-X, Wu Q, Cai L-C, Jin K. Universal cubic equations of state and contact values of the radial distribution functions for multicomponent additive hard-sphere mixtures. *Mol Phys*. 2013;111:3327–3332.
51. de Lonngi DA, Villanueva PAL. Equation of state for small system of hard-spheres. *Rev Mex Fis*. 1992;38:40–58.
52. Clisby N, McCoy BM. Ninth and tenth virial coefficients in D dimensions. *J Stat Phys*. 2006;122:15–57.
53. Tildesley DJ, Streett WB. An equation of state for hard dumbbell fluids. *Mol Phys*. 1980;41:85–94.
54. Yethiraj A, Hall CK. Local structure of fluids containing chain-like molecules: polymer reference site interaction model with a Yukawa closure. *J Chem Phys*. 1990;93:5315–5321.
55. Sadus RJ. Equations of state for hard-sphere chains. *J Phys Chem*. 1995;99:12363–12366.
56. Sadus RJ. A simple equation of state for hard-sphere chains. *AIChE J*. 1999;45:2454–2457.
57. Wu G-W, Sadus RJ. Hard-sphere compressibility factors for equation of state development. *AIChE J*. 2005;51:309–313.
58. Boublik T, Vega C, Diaz-Pena M. Equation of state of chain molecules. *J Chem Phys*. 1990;93:730–736.

Manuscript received Apr. 17, 2014, and revision received Dec. 22, 2014.